



**Non-competitive fluorescence polarization immunosensing
for CD9 detection using a peptide as a tracer**

Journal:	<i>Lab on a Chip</i>
Manuscript ID	LC-ART-03-2022-000224.R1
Article Type:	Paper
Date Submitted by the Author:	24-May-2022
Complete List of Authors:	<p>Takahashi, Kazuki; Hokkaido University, Graduate School of Chemical Sciences and Engineering Chida, Shunsuke; Hokkaido University, Graduate School of Chemical Sciences and Engineering Suwatthanarak, Thanawat; Tokyo Institute of Technology, Department of Chemical Science and Engineering Iida, Mikiko; Nagoya University, Department of Biomolecular Engineering, Graduate School of Engineering Zhang, Min; Nagoya Daigaku, Department of Biomolecular Engineering, Graduate School of Engineering FUKUYAMA, MAO; Tohoku University, Institute of Multidisciplinary Research for Advanced Materials; Maeki, Masatoshi; Hokkaido University, Division of Applied Chemistry, Faculty of Engineering Ishida, Akihiko; Hokkaido University, Division of Applied Chemistry, Faculty of Engineering Tani, Hirofumi; Hokkaido University, Division of Applied Chemistry, Faculty of Engineering Yasui, Takao; Nagoya University, Department of Biomolecular Engineering, Graduate School of Engineering Baba, Yoshinobu; Nagoya University, Department of Biomolecular Engineering, Graduate School of Engineering Hibara, Akihiko; Tohoku University, Institute of Multidisciplinary Research for Advanced Materials Okochi, Mina; Tokyo Institute of Technology, Department of Chemical Science & Engineering Tokeshi, Manabu; Hokkaido University, Division of Applied Chemistry, Faculty of Engineering</p>

Non-competitive fluorescence polarization immunosensing for CD9 detection using a peptide as a tracer

Kazuki Takahashi^a, Shunsuke Chida^a, Thanawat Suwatthanarak^b, Mikiko Iida^c, Min Zhang^c, Mao Fukuyama^d, Masatoshi Maeki^{ef}, Akihiko Ishida^e, Hirofumi Tani^e, Takao Yasui^{cfg}, Yoshinobu Baba^{cg}, Akihide Hibara^d, Mina Okochi^b, Manabu Tokeshi^{eghi}

^a*Graduate School of Chemical Sciences and Engineering, Hokkaido University, Kita 13 Nishi 8, Kita-ku, Sapporo 060-8628, Japan*

^b*Department of Chemical Science & Engineering, Tokyo Institute of Technology, 2-12-2 O-okayama, Meguro-ku, Tokyo 152-8552, Japan*

^c*Department of Biomolecular Engineering, Graduate School of Engineering, Nagoya University, Furo-cho, Chikusa-ku, Nagoya 464-8603, Japan*

^d*Institute of Multidisciplinary Research for Advanced Materials, Tohoku University, 2-1-1 Katahira, Aoba-ku, Sendai 980-8577, Japan*

^e*Division of Applied Chemistry, Faculty of Engineering, Hokkaido University, Kita 13 Nishi 8, Kita-ku, Sapporo 060-8628, Japan. E-mail: tokeshi@eng.hokudai.ac.jp; Tel: +81-11-706-6744; Fax: +81-11-706-6745*

^f*Japan Science and Technology Agency (JST), PRESTO, 4-1-8, Honcho, Kawaguchi, Saitama 332-0012, Japan*

^g*Institute of Nano-Life Systems, Institute of Innovation for Future Society, Nagoya University, Furo-cho, Chikusa-ku, Nagoya 464-8601, Japan*

^h*Innovative Research Center for Preventive Medical Engineering, Nagoya*

University, Furo-cho, Chikusa-ku, Nagoya 464-8601, Japan

*iQuantum Immunology Group, Institute for Quantum Life Science, National
Institutes for Quantum and Radiological Science and Technology (QST), 4-9-1,
Anagawa, Inage-ku, Chiba 263-0024, Japan*

Abstract

This paper is the first report of a non-competitive fluorescence polarization immunoassay (NC-FPIA) using a peptide as a tracer. NC-FPIA can easily and quickly quantify the target after simply mixing them together. This feature is desirable for point-of-need applications such as clinical diagnostics, infectious disease screening, on-site analysis for food safety, etc. In this study, NC-FPIA was applied to detect CD9, which is one of the exosome markers. We succeeded in detecting not only CD9 but also CD9 expressed exosomes derived from HeLa cells. This method can be applied to various targets if a tracer for the target can be prepared, and expectations are high for its future uses.

Introduction

Immunosensing makes it possible to selectively measure a target of interest from biological samples having a complex composition by utilizing the specificity of an antibody.¹ Therefore, many immunosensing devices have been reported so far. In particular, by fusing immunosensing technology with microfluidics, a small amount of sample^{2,3}, rapid analysis and diagnostics^{4,5}, high sensitivity⁶⁻⁸, etc. have been realized. However, most of the devices provide heterogeneous immunoassays, as represented by ELISA, which require antibody immobilization and washing operations that make the analysis operations relatively complicated. On the other hand, homogeneous immunoassays, which can be achieved by simply mixing a sample and reagents in a solution, are not often combined with microfluidics.⁹⁻¹⁴ The desired specifications of sensing differ depending on the measurement target and measurement scene. In some cases, high sensitivity is desired, and in other cases, simple operation is desired. Therefore, it is important to develop sensing technology according to the purpose.

Recently, we have focused on the one of the homogeneous immunoassays, fluorescence polarization immunoassay (FPIA),¹⁵ which offers ease of operation, and we are working on its applications.^{16,17} FPIA is a competitive immunoassay for measuring small molecules using the degree of fluorescence polarization (P) as an index. The P value depends on the rotational movement of a fluorescently labeled target molecule called a tracer in a solution. When the tracer binds to a macromolecule such as an antibody, the rotational movement of the complex is suppressed and the P value changes. The magnitude of the change in P value (ΔP) depends on the change in molecular weight of the tracer before and after

binding to the antibody. In other words, the smaller the molecular weight of the tracer, the larger the ΔP and the higher the sensitivity of assay. Therefore, it is difficult in principle to apply large tracer molecules such as proteins for FPIA. Most recently, we have developed a non-competitive FPIA (NC-FPIA) that can measure large molecules using a fluorescently labeled protein fragment or a fluorescently labeled antibody fragment as a tracer.¹⁸⁻²¹ This method can also be applied to virus detection.²² NC-FPIA is even simpler than conventional FPIA. If a tracer that is fluorescently labeled with a substance that has an affinity for the target can be produced, this method can be applied to the detection of various proteins, antibodies, viruses, and so forth. The sensitivity of NC-FPIA also depends on the change in the molecular weight of the tracer before and after binding to the target, as in the conventional FPIA. The tracers we have prepared so far are a H5 hemagglutinin fragment (~30 kDa) for anti-H5 avian influenza antibody detection,¹⁸ a VHH antibody (~15 kDa) for rabbit IgG detection,¹⁹ Fab fragments (~50 kDa) for C-reactive protein (CRP) detection²⁰ and avian influenza virus (H5N3) detection,²² and a spike protein fragment (~39 kDa) for anti-SARS-CoV-2 antibody detection.²¹

On the other hand, peptides have been widely studied as drugs for metabolic and tumor related diseases²³ and as valuable tools for diagnostic applications.²⁴ So far, many peptides with high affinity for targets have been developed for various purposes. Some peptides have a high affinity comparable to that of antibodies. These peptides have a smaller molecular weight than VHH antibodies and can be expected to be excellent tracers for NC-FPIA. However, NC-FPIA using peptides as tracers has not been reported so far, and

investigation of its potential, especially to bioapplications, is highly desired.

In this study, we applied NC-FPIA, which uses a peptide (~1.5 kDa) as a tracer, to detect CD9, an exosome marker protein.²⁵ This is the first report of NC-FPIA using a peptide tracer. Exosomes are extracellular vesicles secreted by most cell types and are thought to be responsible for cell-to-cell communication.²⁶ Since exosomes contain biological information about diseases such as cancer, they are expected to be potential cancer biomarkers.²⁷ The exosomal membrane is enriched with endosome-specific tetraspanins CD9, CD63, and CD81, which are used to detect exosomes.²⁸ Dedicated ELISA kits and equipment have been developed for the detection of tetraspanins, but they have problems such as complicated operations, time-consuming measurements, and high cost. The detection of CD9 by NC-FPIA that we propose here can detect CD9 quickly without the need for antibody immobilization or washing operations. In fact, we have succeeded in detecting CD9 on the membrane surface of exosomes derived from cultured cells, demonstrating that this new immunosensing method can also contribute to the study of exosomes.

Experimental section

Chemicals

All reagents were used without purification. Phosphate-buffered saline (PBS; pH 7.4) and fluorescein-5-isothiocyanate (FITC 'Isomer I') were obtained from Thermo Fisher Scientific, Inc. (USA). Albumin from bovine serum (BSA) was purchased from FUJIFILM Wako Pure Chemical Corporation (Japan). Recombinant human CD9 was purchased from Proteintech Group, Inc (USA).

Dulbecco's modified Eagle's medium-high glucose (DMEM) was purchased from Sigma-Aldrich Corp. (USA). Fetal bovine serum (FBS) and 1% penicillin/streptomycin were purchased from Gibco (USA).

Instruments

For the fluorescence polarization measurement, a previously developed compact fluorescence polarization apparatus was used as described in detail elsewhere.^{16,29} The microfluidic device which had nine channels was fabricated using the standard soft lithography technique.³⁰ Black PDMS was used to reduce background fluorescence.¹⁶ The device was manufactured by adhering a black PDMS with microchannel structures onto a glass substrate. Each microchannel in the measurement area was 200 μm wide and 900 μm deep (Fig. 1). A resin interface was formed with a 3D printer (AGLISTA-3110, Keyence (Japan)) and inserted into the device inlet so that the sample could be easily introduced into the microchannel. The sample volume of each microchannel was approximately 20 μL . The concentration and size of extracellular vesicles (EVs) was measured using a nanoparticle tracking analysis system (NTA) (NanoSight LM10, Malvern Panalytical (Netherlands)), and the expression levels of membrane proteins of EVs were measured with an ExoView R100 (NanoView Biosciences (USA)).

Preparation of tracers

We recently reported the synthesis and screening for an antimigratory peptide with the CD9 binding property.³¹ Separately, we determined the dissociation

constant (K_d) of CD9 binding peptide (CD9 BP)-CD9 complex was 4.66×10^{-7} M. The CD 9 BP preferentially bound to CD9 rather than to the other exosome membrane proteins.³² In this study, FITC-labeled CD9 binding peptide (RSHRLRLH) (F-CD9 BP) was used as a tracer. To assess tracer performance, AAAA peptide was also labeled with FITC (F-AAAA P) (a negative control). The details of CD9 BP synthesis, screening, and labeling were the same as previously used.³¹

Non-competitive fluorescence polarization immunoassay (NC-FPIA) of CD9

A 10 μ M F-CD9 BP/PBS solution was prepared with PBS to a concentration of 1.25, 2.5, 5.0, or 10 nM. The CD9 stock solution was adjusted to 250 μ g/mL by dissolving the powder in PBS according to the manufacturer's protocol, and each concentration of CD9 solution was prepared by serial dilution. A 10 μ M F-AAAA P/PBS solution was prepared with PBS to 2.5 nM. For CD9 measurements, PBS, CD9, F-CD9 BP or F-AAAA P, and 1% BSA-PBS were added to a 0.5 mL microtube with the mixing volume ratio of PBS: CD9: F-CD9 BP or F-AAAA P: 1% BSA-PBS = 60:20:10:10. Total volume of the final mixed solution was 100 μ L. Then, after incubating the mixed solution at 25 °C for 30 min, 20 μ L of solution was introduced into the microdevice, and the P value was measured with the compact fluorescence polarization apparatus.

Preparation of exosomes derived from cultured cells and NC-FPIA

HeLa cells were cultured with DMEM containing 10% FBS and 1% penicillin/streptomycin. HeLa cells were maintained at 37 °C in a humidified

incubator with 5% CO₂. The cells were washed with PBS, and the culture medium was replaced with advanced DMEM, not including FBS and 1% penicillin/streptomycin. After incubation for 48 h, the culture supernatant was collected and centrifuged at 300 × *g* for 10 min at 4 °C. The centrifuged supernatant was centrifuged at 200 × *g* for 10 min at 4 °C, again. To thoroughly remove cellular debris, the supernatant was filtered through a 0.22 μm filter (Merck Millipore Corp.). The supernatant was ultracentrifuged at 110000 × *g* for 80 min at 4 °C. After discarding the supernatant, the precipitants (EV pellets) were washed by 0.22-μm filtered PBS. The PBS was ultracentrifuged at 110000 × *g* for 80 min at 4 °C, again. After discarding the supernatant, the EV pellets were suspended in 0.22-μm filtered PBS. For the measurement of CD9 expressed exosomes, the sample was prepared by diluting the suspension with PBS. The measurement of the *P* value was the same as described above.

Results and discussion

Optimization conditions and performance evaluation for NC-FPIA of CD9

The biggest advantage of our NC-FPIA is its simplicity. By simply mixing the tracer and the sample, the concentration of the target to be measured in the sample can be quantified. Schematic illustrations of the NC-FPIA of CD9 are shown in Figure 2 (a, b). *P* value varies depending on the amount of F-CD9 BP-CD9 complex in the mixture. If the amount of F-CD9 BP in the mixture is kept constant, the *P* value changes according to the amount of CD9, and the concentration of CD9 can be quantified using the *P* value as an index. In order to optimize the reaction conditions between CD9 and the tracer (F-CD9 BP), the

concentration of CD9 was fixed at 8 μM and the F-CD9 BP concentration was changed to measure the degree of fluorescence polarization (P value). Figure 3 shows the F-CD9 BP concentration dependence on ΔP . ΔP is the difference of the P value between the maximum value and the blank. From the results of the experiment, we found that the highest ΔP was 2.5 nM. Therefore, we selected 2.5 nM as an optimal tracer concentration for our further experiments on NC-FPIA of CD9.

Next, we measured the CD9 concentration dependence on ΔP (Figure 4). ΔP increased with increasing CD9 concentration, indicating that the F-CD9 BP was quantitatively bound to CD9. The results of the reaction of 2.5 nM F-AAAA P and CD9 are also shown in Figure 3 to evaluate the selectivity of the reaction between the F-CD9 BP and CD9. As clearly seen from the figure, F-AAAA P did not bind to CD9 at all, and F-CD9 BP did selectively bind to CD9. The limit of detection (LOD) of CD9 was evaluated to be 300 nM, considering the average of the blank signal plus three standard deviations. This is the first example of NC-FPIA using a peptide tracer. The CD9 BP used this time has the dissociation constant of 4.66×10^{-7} M in the complex with CD9, so its affinity is not so high.³² In the future, we expect the sensitivity of this method will be increased by synthesizing peptides with higher affinity.³³ In this study, the measurement of the high concentration region of CD9 was not done in consideration of reagent consumption and cost, but we could estimate it. Assuming that the shape of the tracer is spherical, we can express the P value by the following equation:^{19,20,34}

$$P = \frac{M_W}{\frac{1}{P_0}M_W + \frac{(3 - P_0)(RT\tau)}{3\eta P_0(V + h)}} \quad (1)$$

where M_W is the molecular weight, P_0 is the polarization without rotation diffusion, R is the gas constant, T is temperature τ is the fluorescence lifetime of the fluorophore, η is the medium viscosity, V is the partial specific volume, and h is the degree of hydration. Therefore, ΔP can be obtained using the following equation:

$$\Delta P = P_{\text{complex}} - P_{\text{F-CD9 BP}} \quad (2)$$

where P_{complex} and $P_{\text{F-CD9 BP}}$ are the P values of the F-CD9 BP-CD9 complex and F-CD9 BP, respectively. For the calculation of ΔP , we used the values M_W (complex) = 16,462 g/mol, M_W (F-CD9 BP) = 1,462 g/mol, $P_0 = 0.531$,³⁵ $T = 298.15$ K, $\tau = 4.0$ ns,³⁵ $\eta = 0.89$ cP,³⁶ $V = 0.74$ mL/g,³⁵ and $h = 0.20$ mL/g.^{35,37} ΔP obtained by substituting these values was 0.0247 (247 mP). Considering this value and the behavior of ΔP seen in Figure 4, the high concentration region of CD9 seemed to be saturated at about 100 μM . Therefore, we considered the developed NC-FPIA method has a dynamic range of 2 orders or more of magnitude.

Measurement of CD9 expressed exosomes

Since we succeeded in detecting CD9 by the NC-FPIA method using the developed peptide tracer, we then applied this method to the detection of CD9 expressed exosomes (Figure 2 (c)). Exosomes measured as shown in the experimental section were obtained by ultracentrifugation of the supernatant of the HeLa cell culture medium. The EV particle size distribution of the sample obtained by ultracentrifugation was measured by NTA (Figure 5 (a)). From this result, we found that the sample contained 1.34×10^{12} particles/mL of EVs.

These EVs included exosomes that express the tetraspanin membrane proteins and small EVs that do not. The amount of CD9 expressed exosomes in the sample was measured using the Exoview and found to be 5.03×10^9 particles/mL (Figure 5 (b)). Using this sample, we carried out NC-FPIA of CD9 expressed exosomes.

Figure 6 shows the results of the detection ability test for CD9 expressed exosomes using the dilution samples. As a negative control, the results of using F-AAAA P as a tracer instead of F-CD9 BP are also shown. The ΔP decreased according to the dilution rate of the sample, and we found that CD9 expressed exosomes could be detected by this method up to $\times 1000$. Since the ΔP of $\times 10000$ was about the same as that of the blank and the CD9 expressed exosomes have not been detected, the detection limit of this method was judged to be about $\times 1000$. This result seems reasonable considering the following: multiple CD9s are expressed on one exosome and the dissociation constant of CD9-CD9 BP on exosomes is lower than that in solution due to the stabilization of CD9 by the lipid membrane. Furthermore, the CD9 BP used this time has been reported to bind slightly to other proteins such as EpCAM and integrin $\beta 5$ on exosomes.³² On the other hand, ΔP was not as large as expected as discussed earlier. The molecular weight of the exosome is unknown, but the molecular weight of the F-CD9 BP-CD9 exosome complex is clearly much larger than that of the F-CD9 BP-CD9 complex in solution. However, ΔP was only 18.7 mP for $\times 10$, 16.7 mP for $\times 100$, and 11.7 mP for $\times 1000$ sample. A similar tendency for ΔP , which is much smaller than expected, has been observed in virus detection using antibody fragments such as Fab²² and scFV³⁸ as tracers.

For large targets such as particles and viruses, it seems that the theoretical calculation of P values must be modified or reconstructed. Currently, the reasons for this are unknown; however, it is an interesting issue from the perspective of quantifying fluorescence polarization of large targets.

We have succeeded in detecting exosomes by the NC-FPIA method using peptides as tracers, although there are some points that need to be clarified. This NC-FPIA measurement is very simple: mix the sample and tracer, incubate for 30 min, then introduce the mixture into the device and measure the degree of fluorescence polarization. In addition, the assay time is short and there is no need for troublesome procedures such as the washing required for ELISA kit and Exoview measurements. Furthermore, although we detected only CD9 this time, we expect that simultaneous detection of CD9, CD63, and CD81 on exosomes will be possible if tracers for CD63 and CD81 and labeled fluorescent dyes with different fluorescence wavelengths are developed.

Conclusion

In this study, we conducted NC-FPIA using peptides as tracers for the first time and demonstrated the sensing ability of this approach. With the simple operation of mixing the tracer and the sample, we succeeded in detecting CD9 and CD9 expressed exosomes in samples. In the future, this method can be improved in performance and functionality by developing peptides with higher affinity and peptides that recognize other proteins. In fact, peptides with affinities for important biological proteins have been synthesized and screened by other researchers³⁹ and they can be applied to this method. Although there

is room for improvement in sensitivity and selectivity, NC-FPIA, which can detect exosomes easily and quickly, has great potential as a detection technology not only for exosomes but also for small EVs expressing specific proteins.

Author contributions

Kazuki Takahashi: investigation, visualization, and writing-original draft. Shunsuke Chida: investigation and visualization. Thanawat Suwatthanarak: investigation and resources. Mikiko Iida: investigation and resources. Min Zhang: investigation and resources. Mao Fukuyama: methodology, resources, and discussion. Masatoshi Maeki: methodology, resources, and discussion. Akihiko Ishida: methodology, investigation, and discussion. Hirofumi Tani: methodology, investigation, and discussion. Takao Yasui: investigation and resources. Yoshinobu Baba: investigation and resources. Akihide Hibara: methodology, resources, and discussion. Mina Okochi: resources, and writing - and review & editing. Manabu Tokeshi: methodology, and writing – review & editing, supervision, project administration, funding acquisition.

Conflicts of interest

There are no conflicts to declare.

Acknowledgements

This work was supported by AMED Grant Number JP21zf0127004, JSPS KAKENHI (Grant Numbers: JP21H01726 and JP21H01960), JST PREST (JPMJPR19H9) and the Cooperative Research Program of “Network Joint

Research Centre for Materials and Devices”.

References

1. The Immunoassay Handbook, 4th edn, ed. D. Wild, Elsevier, Amsterdam, 2013
2. M. Ikami, A. Kawakami, M. Kakuta, Y. Okamoto, N. Kaji, M. Tokeshi and Y. Baba, *Lab Chip*, 2010, **10**, 3335-3340
3. Z. Swank, G. Michielin, H. M. Yip, P. Cohen, D. O. Andrey, N. Vuilleumier, L. Kaiser, I. Eckerle, B. Meyer and S. J. Maerkl, *Proc. Natl. Acad. Sci. USA*, 2021, **118**, e2025289118.
4. T. Ohashi, K. Mawatari, K. Sato, M. Tokeshi, T. Kitamori, *Lab Chip*, 2009, **9**, 991-995
5. V. Sunkara, S. Kumar, J. Sabaté del Rio, I. Kim and Y. -K. Cho, *Acc. Chem. Rec.*, 2021, **54**, 3643-3655.
6. S. H. Kim, S. Iwai, S. Araki, S. Sakakihara, R. Iino and H. Noji, *Lab Chip*, 2012, **12**, 4986-4991
7. Y. Yang and Y. Zeng, *Lab Chip*, 2018, **18**, 3830-3839.
8. V. Yelleswarapu, J. R. Buser, M. Haber, J. Baron, E. Inapuri and D. Issadore, *Proc. Natl. Acad. Sci. U.S.A*, 2019, **116**, 4489-4495
9. A. Hatch, A. E. Kamholz, K. R. Hawkins, M. S. Munson, E. A. Schilling, B. H. Weigl and P. Yager, *Nat. Biotechnol.*, 2001, **19**, 461-465
10. T. Tachi, N. Kaji, M. Tokeshi and Y. Baba, *Lab Chip*, 2009, **9**, 966-971
11. T. Tachi, N. Kaji, M. Tokeshi and Y. Baba, *Anal. Sci.*, 2009, **25**, 149-151
12. T. Tachi, T. Hase, Y. Okamoto, N. Kaji, T. Arima, H. Matsumoto, M. Kondo, M. Tokeshi, Y. Hasegawa and Y. Baba, *Anal. Bioanal. Chem.*, 2011, **401**, 2301-2305

13. J. -W. Cho, D. -K. Kang, H. Park, A. J. deMello and S. -I. Chang, *Anal. Chem.*, 2012, **84**, 3849-3854.
14. K. Nishiyama, K. Sugiura, N. Kaji, M. Tokeshi and Y. Baba, *Lab Chip*, 2019, **19**, 233-240
15. O. H. Hendrickson, N. A. Taranova, A. V. Zherdev, B. B. Dzantiev and S. Eremin, *Sensors*, 2020, **20**, 7132
16. O. Wakao, K. Satou, A. Nakamura, P. A. Galkina, K. Nishiyama, K. Sumiyoshi, F. Kurosawa, M. Maeki, A. Ishida, H. Tani, M. A. Proskurnin, K. Shigemura, A. Hibara and M. Tokeshi, *Lab Chip*, 2019, **19**, 2581-2588
17. A. Nakamura, M. Aoyagi, M. Fukuyama, M. Maeki, A. Ishida, H. Tani, K. Shigemura, A. Hibara and M. Tokeshi, *ACS Food Sci. Technol.*, 2021, **1**, 1623-1628
18. K. Nishiyama, Y. Takeda, M. Maeki, A. Ishida, H. Tani, K. Shigemura, A. Hibara, Y. Yonezawa, K. Imai, H. Ogawa, M. Tokeshi, *Sens. Actuators B*, 2020, **316**, 128160
19. M. Fukuyama, A. Nakamura, K. Nishiyama, A. Imai, M. Tokeshi, K. Shigemura, A. Hibara, *Anal. Chem.*, 2020, **92**, 14393-14397
20. K. Nishiyama, M. Fukuyama, M. Maeki, A. Ishida, H. Tani, A. Hibara, M. Tokeshi, *Sens. Actuators B*, 2021, **326**, 128982
21. K. Nishiyama, K. Takahashi, M. Fukuyama, M. Kasuya, A. Imai, T. Usukura, N. Maishi, M. Maeki, A. Ishida, H. Tani, K. Hida, K. Shigemura, A. Hibara, M. Tokeshi, *Biosens. Bioelectron.*, 2021, **190**, 113414
22. K. Nishiyama, Y. Takeda, K. Takahashi, M. Fukuyama, M. Maeki, A. Ishida, H. Tani, K. Shigemura, A. Hibara, H. Ogawa, M. Tokeshi, *Anal. Bioanal.*

- Chem.*, 2021, **413**, 4619-4623
23. A. C.-L. Lee, J. L. Harris, K. K. Khanna, J.-H. Hong, *Int. J. Mol. Sci.*, 2019, **20**, 2383
24. S. Pandey, G. Malviya, M. C. Dvorakova, *Int. J. Mol. Sci.*, 2021, **22**, 8828
25. C. Théry, L. Zitvogel, S. Amigorena, *Nat. Rev. Immunol.*, 2002, **2**, 569-579
26. S. L. N. Maas, X. O. Breakefield, A. M. Weaver, *Trends Cell Biol.*, 2017, **27**, 172-188
27. T. Yasui, T. Yanagida, S. Ito, Y. Konakade, D. Takeshita, T. Naganawa, K. Nagashima, T. Shimada, N. Kaji, Y. Nakamura, I. A. Thiodorus, Y. He, S. Rahong, M. Kanai, H. Yukawa, T. Ochiya, T. Kawai, Y. Baba, *Sci. Adv.*, 2017, **3**, e1701133
28. C. Campos-Silva, H. Suárez, R. Jara-Acevedo, E. Linares-Espinós, L. Martinez-Piñeiro, M. Yáñez-Mó, M. Valés-Gómez, *Sci. Rep.*, 2019, **9**, 2042
29. O. Wakao, K. Satoh, A. Nakamura, K. Sumiyoshi, M. Shirokawa, C. Mizokuchi, K. Shiota, M. Maeki, A. Ishida, H. Tani, K. Shigemura, A. Hibara, M. Tokeshi, *Rev. Sci. Instrum.*, 2018, **89**, 024103
30. J. C. McDonald, G. M. Whitesides, *Acc. Chem. Res.*, 2002, **35**, 491-499
31. T. Suwatthanarak, M. Tanaka, Y. Miyamoto, K. Miyado, M. Okochi, *Chem. Commun.*, 2021, **57**, 4906-4909
32. T. Suwatthanarak, I. Adiyasa Thiodorus, M. Tanaka, T. Shimada, D. Takeshita, T. Yasui, Y. Baba, M. Okochi, *Lab Chip*, 2021, **21**, 597-607
33. K. Xu, Y. Jin, Y. Li, Y. Huang, R. Zhao, *Front. Chem.*, 2022, **10**, 844124
34. W. B. Dandliker, V. A. de Saussure, *Immunochemistry*, 1970, **7**, 799-828
35. D. M. Jameson, S. E. Seifried, *Methods*, 1999, **19**, 222-223

36. J. W. Thompson, T. J. Kaiser, J. W. Jorgenson, *J. Chromatogr. A.*, 2006, **1134**, 201-209
37. H. Szmecinski, E. Terpetschnig, J. R. Lakowicz, *Biophys. Chem.*, 1996, **62**, 109-120
38. K. Takahashi, S. Chida, M. Fukuyama, M. Maeki, A. Ishida, H. Tani, A. Hibara, M. Tokeshi, unpublished data.
39. A. J. Quartararo, Z. P. Gates, B. A. Somsen, N. Hartrampf, X. Ye, A. Shimada, Y. Kajihara, C. Ottmann, B. L. Pentelute, *Nat. Commun.*, 2020, **11**, 3182

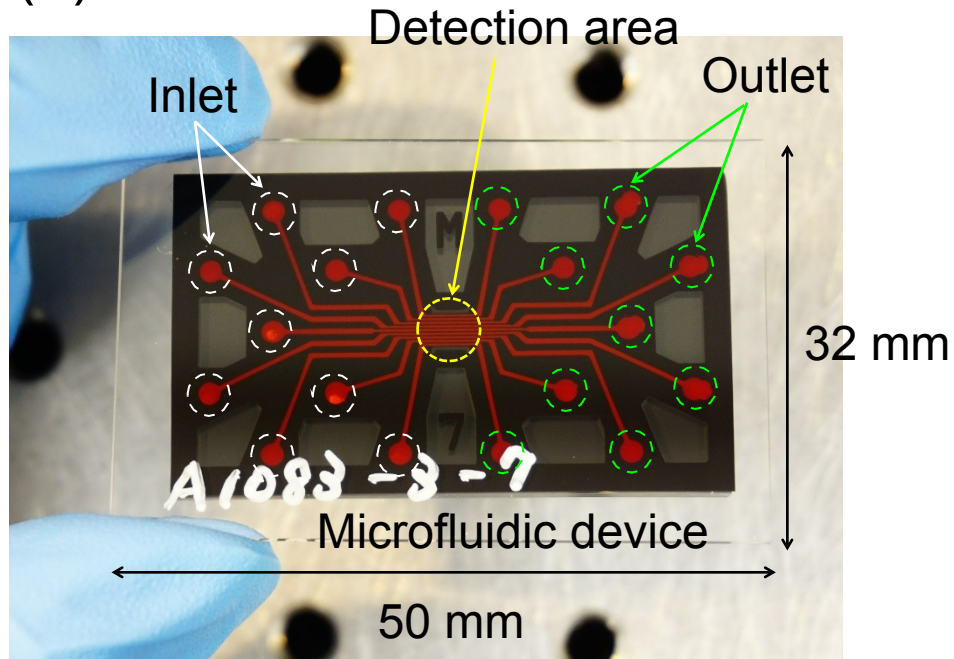
Figure captions

- Figure 1 Photos of (a) the microfluidic device and (b) the microfluidic device with a 3D printed interface for sample introduction. Red ink was introduced into the microchannels to make them easier to see.
- Figure 2 Schematic illustration of the principle of NC-FPIA. When there are a lot of unbound tracer molecules in a sample, the fluorescence is depolarized. On the contrary, when most tracer molecules are bound to the target molecules, fluorescence is polarized. The situation of the sample in the detection of CD9s (a) when there are a few CD9 species present and (b) when there are many CD9 species present. The situation of the sample in the detection of CD9 expressed exosomes (c) when there are many CD9 expressed exosome present.
- Figure 3 F-CD9 BP concentration dependence on ΔP . ΔP is the difference of the P value between the maximum value and the blank. mP means $10^{-3} \times P$. The concentration of CD9 was constant at 8 μM . Each bar represents the mean of triplicate measurements, and the error bar represent standard deviations.
- Figure 4 CD9 concentration dependence on ΔP . The concentration of F-CD9 BP and F-AAAA P was 2.5 nM.
- Figure 5 (a) Size distribution of extracellular vesicles (EVs) measured by NTA in an ultracentrifuged sample of cultured cell supernatant. The pink bars indicate the EV concentration at each EV size; light

pink are error bars. Error bars show the standard deviation for a series of measurements ($n = 5$). (b) EV membrane protein expression levels measured by Exoview R100. CD63, CD81, and CD9 below the line represent antibodies immobilized on the substrate, while CD63, CD81, CD9, and IgG above the line represent fluorescently labeled detection antibodies. For example, CD81 above the line for CD63 represents the number of particles detected when EVs captured by the CD63 immobilized antibody are detected by CD81. Each plot represents the data measured, bars represent mean values, and error bars show the standard deviation for a series of measurements ($n = 3$).

Figure 6 NC-FPIA results for the detection ability test of CD9 expressed exosomes using the dilution samples. Each bar represents the mean of triplicate measurements, and the error bar represent standard deviations.

(a)



(b)

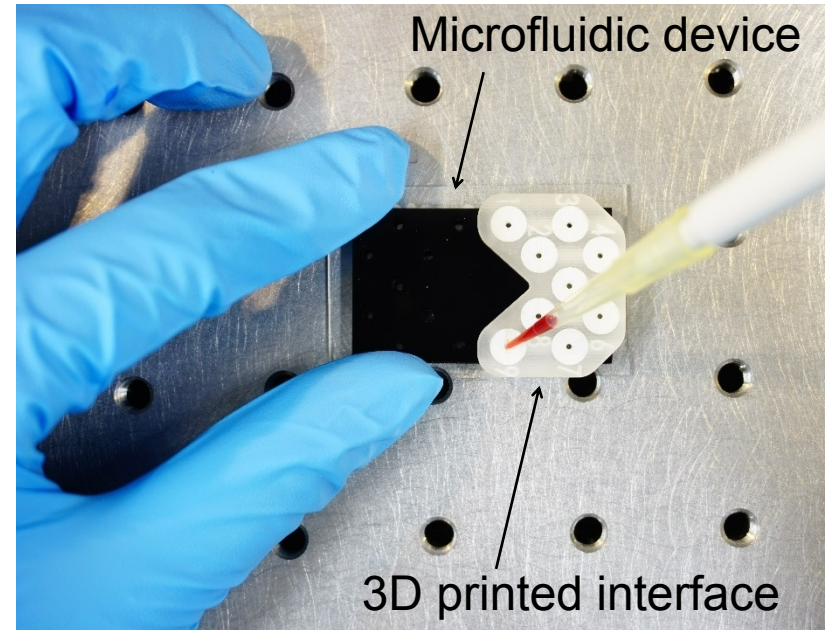


Figure 1

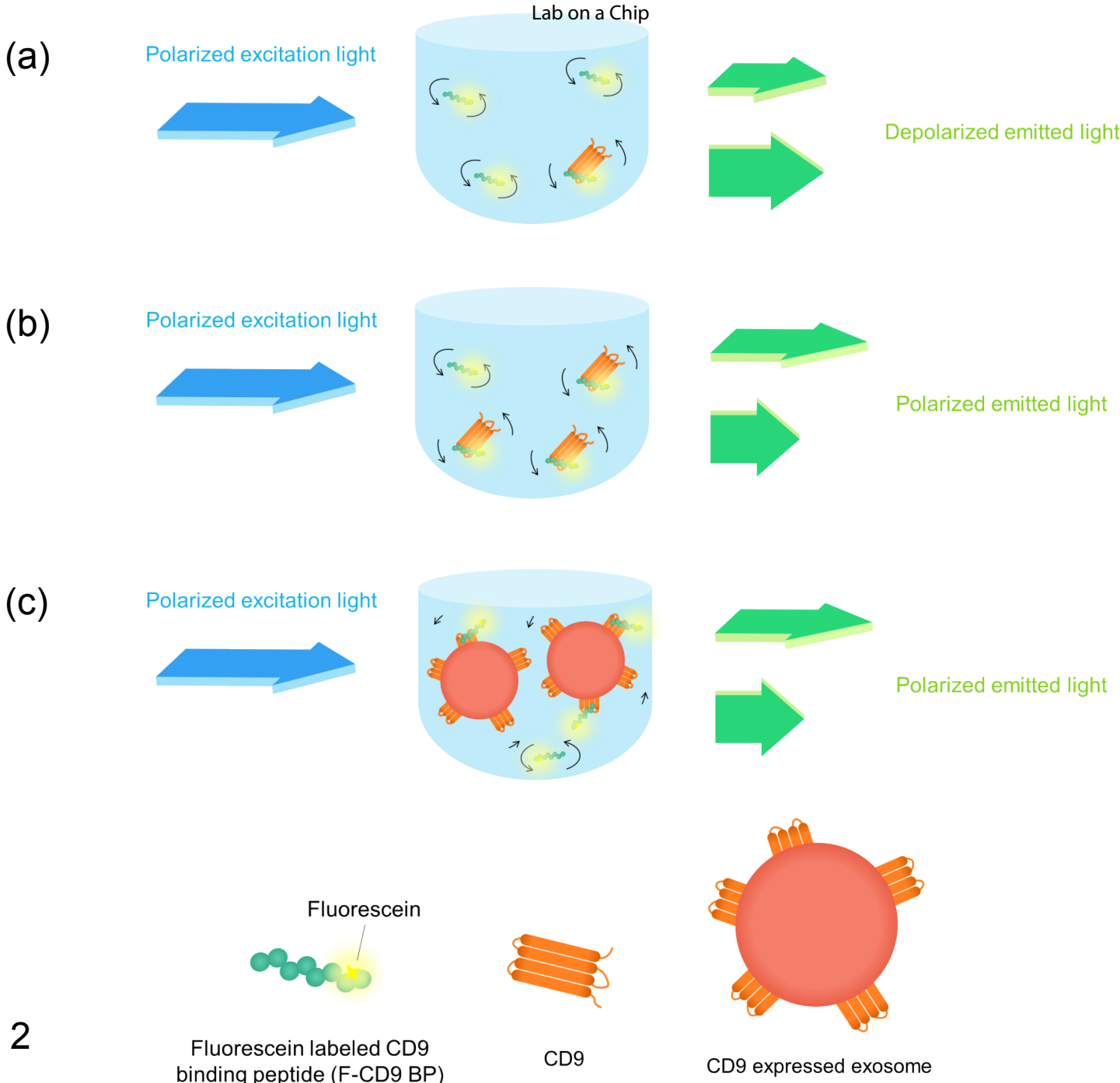


Figure 2

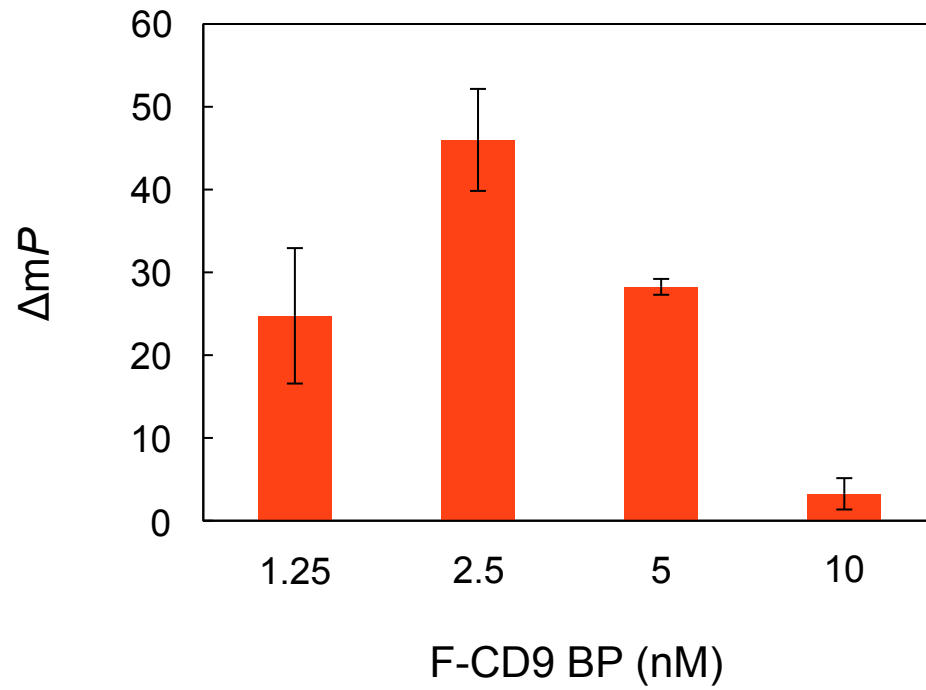


Figure 3

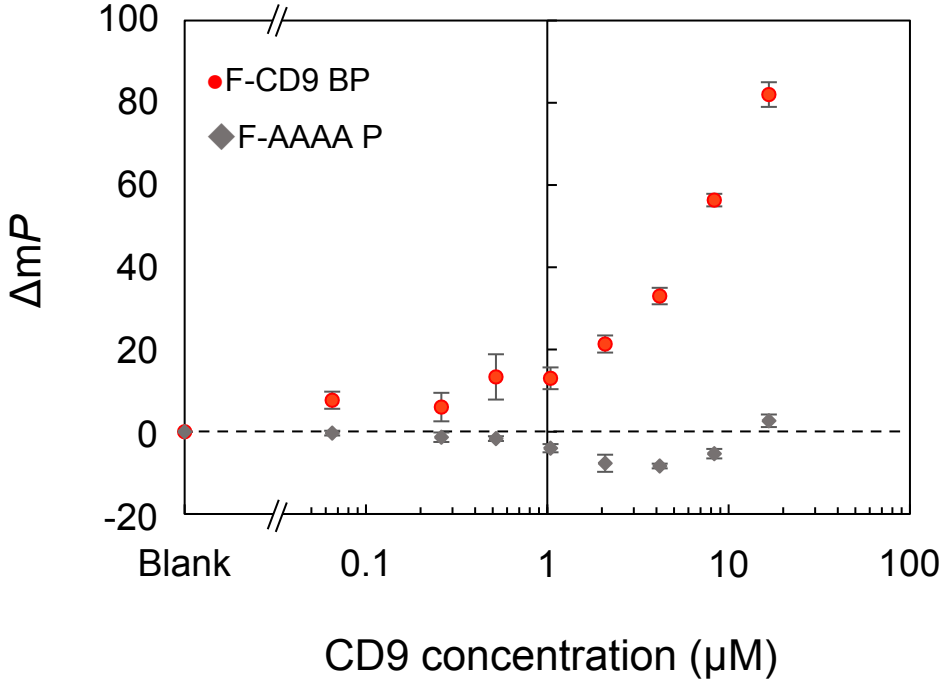


Figure 4

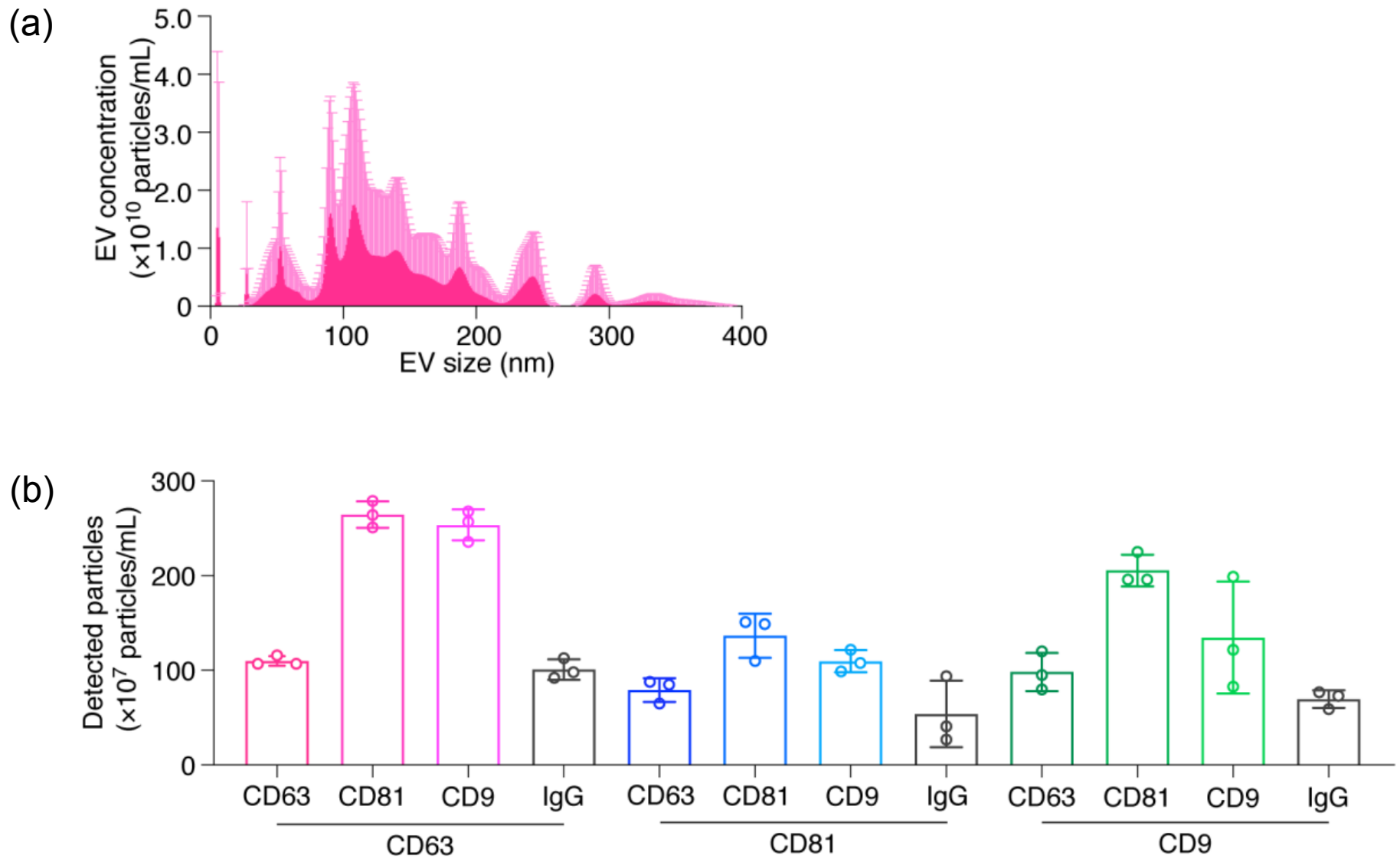


Figure 5

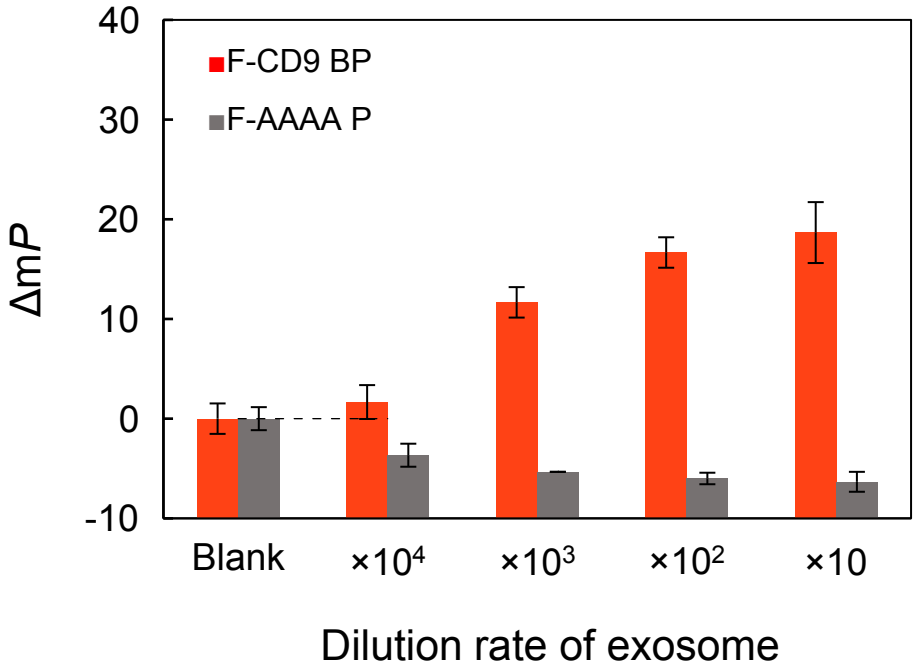


Figure 6